Available online at www.sciencedirect.com
ScienceDirect
Journal of the European Ceramic Society 32 (2012) 1–8
www.elsevier.com/locate/jeurceramsoc

High temperature deformation of ceramic particle composites

Marek Boniecki *, Zdzisław Librant, Władysław Wesołowski

Institute of Electronic Materials Technology, 133 Wólczyńska Str., 01-919 Warsaw, Poland

Received 8 March 2011; received in revised form 8 June 2011; accepted 2 July 2011
Available online 19 August 2011

Abstract

The particle composites Al_2O_3/(2 and 3Y)TZP and $MgAl_2O_4$/3Y-TZP were tested in bending at temperature of 1280 °C over strain rates from 3.4×10^{-7} to 1×10^{-4} s^{-1} and over stresses from 23 to 85 MPa. Strain rate of the composites decreased as a volume fraction of Al_2O_3 or $MgAl_2O_4$ increased. $MgAl_2O_4$/3Y-TZP composites deformed easier under the comparable conditions than alumina/zirconia composites. Four models of composite creep behaviour were compared to the experimental data. All the models were unsuitable for $MgAl_2O_4$/3Y-TZP, in turn an isostress, an isostrain and a constrained isostrain models provide the good predictions for creep rates for alumina/zirconia ceramics, but the rheological model appeared not good. The threshold stresses approach seems to be useful for describing superplastic flow of $MgAl_2O_4$/3Y-TZP composites.

Keywords: Superplasticity; Bending test; Strain rate; Composite; Tetragonal ZrO_2; Threshold stress

1. Introduction

Chemical and thermal stability, relatively good strength and fracture toughness, thermal and electrical insulation characteristics of alumina (Al_2O_3) combined with availability in abundance and low cost of the material resources are advantageous for commercial engineering applications of this ceramics.[1] In turn magnesium aluminate spinel ($MgAl_2O_4$) seems to be a good candidate ceramics for nuclear applications.[2] Spinel shows high resistance to the formation of defects under the influence of neutron irradiation and hence the change in mechanical properties is not critical. However in some applications the strength and fracture toughness of alumina and spinel are not sufficient. In these case zirconia (ZrO_2) particles are frequently employed as toughening agents for these ceramics.[3–6] Zirconia has three crystallographic forms, namely: monoclinic (m), tetragonal (t) and cubic (c) phases.[7,8] The transformation of pure zirconia from t-phase to m-phase occurs at a temperature about 950 °C, which is accompanied by a volume expansion of 4%. This volume expansion generates stresses which prohibit the opening of an advancing crack, so the toughness of zirconia at room temperature is high compared with other ceramics. The phase transformation temperature from t to m can be lowered by doping with suitable oxides such as Y_2O_3, CeO_2 CaO, MgO, etc. For grain size lower that a critical size t-phase at room temperature is stable. Zirconia stabilized by 2–3 mol% Y_2O_3 consists almost 100% tetragonal phase.[7,8] These ceramics attained strength about 1.5 GPa[7] and fracture toughness about[6] 7 MP $am^{1/2}$ and therefore they are mainly used as toughening components in the mentioned above ceramics. It should be also noticed that the composite consisting of 80 wt% ZrO_2 (stabilized by 2 mol% Y_2O_3) and 20 wt% Al_2O_3 (28 vol%) attained strength values about 2.5 GPa (after hot isostatic pressing in the last stage of manufacture).[8] Then it is a great interest of application of the ceramic materials in some tools and engine parts production but obtaining of ceramic elements is not easy and cheap because of brittleness and hardness of ceramics at room temperature. To some extent an opportunity of easy shaping and joining of them is created by superplasticity. This phenomenon, well known in metallic materials,[9] was demonstrated for the first time for ceramic materials for 3 mol% Y_2O_3 stabilized tetragonal ZrO_2 in 1985 in Japan by Wakai et al. The publication of the results of their work took place in 1986.[10] Since then many articles concerning superplasticity in ceramics have been published. Some of them describe superplastic flow in tetragonal zirconia,[11–13] alumina,[14] $MgAl_2O_4$ spinel,[15] alumina–zirconia[16–18] and spinel–zirconia composites.[19,20] These composites are an object of the main interest of this paper. In the present investigation, the influence of

* Corresponding author.
E-mail addresses: Marek.Boniecki@itme.edu.pl, Marek-Boniecki@wp.pl (M. Boniecki).

0955-2219/$ – see front matter © 2011 Elsevier Ltd. All rights reserved.
doi:10.1016/j.jeurceramsoc.2011.07.001

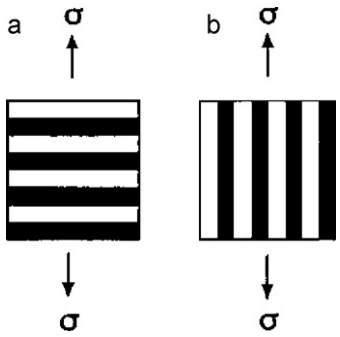

Fig. 1. Schematic diagram showing (a) isostress and (b) isostrain model.

alumina and spinel volume fraction on strain rate of Al_2O_3/ZrO_2 and $MgAl_2O_4/ZrO_2$ particulate composites at 1280 °C in bending test is studied. These experimental conditions were chosen in order to avoid of grain size growth or cavitation nucleation during the test. For comparison, in[12–20] the compression and tensile tests were made at temperatures usually higher than 1280 °C and hence a strain reached there about several hundred percent, but in our case it does not exceed 2%.

2. Theoretical background

The creep and superplasticity in the material can be described by the following equation[11–14]:

$$\dot{\varepsilon} = \frac{A_0 DGb}{kT}\left(\frac{b}{d}\right)^p\left(\frac{\sigma}{G}\right)^n \tag{1}$$

where $\dot{\varepsilon} = d\varepsilon/dt$ is the strain rate, A_0 is a dimensionless constant, D is the diffusion coefficient [$=D_0 exp(-Q/RT)$, where D_0 is the frequency factor, Q the activation energy and R the gas constant], σ is the applied stress, G is the shear modulus, b is the Burgers vector, d is the grain size, k is Boltzmann's constant, p is the inverse grain size exponent and n is the stress exponent.

In order to describe two-phase particle composite behaviour several models were proposed.[21,22] Two of them, so-called isostress and isostrain model,[21] based on the standard composite theory (rule of mixture -ROM). The third, so-called rheological model,[22] based on assumption that one phase is rigid and the other is deformable. ROM models (Fig. 1) assume that the duplex microstructure can be simplified to one that consists of plates of each phase. Two conditions can be fulfilled: (a) isostress (plates are aligned perpendicular to the applied stress), where the stress is the same in each phase, and (b) isostrain (where the plates are parallel to the applied stress), where the strain and strain rate are the same for each phase.

The composite strain rate for isostress case is given by the relation

$$\dot{\varepsilon} = V_1\dot{\varepsilon}_1 + (1 - V_1)\dot{\varepsilon}_2 \tag{2}$$

where V_1 and $\dot{\varepsilon}_1$ are the volume fraction and strain rate of component one and $(1 - V_1)$ and $\dot{\varepsilon}_2$ are the volume fraction and strain rate of component two.

The stress in the composite for isostrain case is given by the relation

$$\sigma = V_1\sigma_1 + (1 - V_1)\sigma_2 \tag{3}$$

Assuming that each component obeys Eqs. (1) and (3) is given by

$$\sigma = V_1 K_1 \dot{\varepsilon}^{1/n_1} + (1 - V_1)K_2\dot{\varepsilon}^{1/n_1} \tag{4}$$

where $K_i = G(kT/A_0 DGb)^{1/n_i}(d/b)^{p/n_i}$ for each component i.

An analytical solution of Eq. (4) for $\dot{\varepsilon}$ as a function of V_1 is not possible for $n_1 \neq n_2$. However Eq. (4) can be rearranged to provide a solution for V_1 as a function of $\dot{\varepsilon}$ as

$$V_1 = \frac{\sigma - K_2\dot{\varepsilon}^{1/n_2}}{K_1\dot{\varepsilon}^{1/n_1} - K_2\dot{\varepsilon}^{1/n_2}} \tag{5}$$

So the values of $\dot{\varepsilon}$ which give $0 < V_1 < 1$ are those of interest. These are the values which fall between $\dot{\varepsilon}_1$ and $\dot{\varepsilon}_2$ for the given applied stress. It is then a matter of determining the values of V_1 as a function of $\dot{\varepsilon}$, then plotting $\dot{\varepsilon}$ as a function of V_1.

By assuming that the stress exponents in each phase are equal (i.e. $n = n_1 = n_2$ – constrained isostrain model[18]), Eq. (4) can be simplified and written in the terms of the composite strain rate, $\dot{\varepsilon}$:

$$\dot{\varepsilon} = \frac{\sigma^n}{(V_1 K_1 + (1 - V_1)K_2)^n} \tag{6}$$

In the rheological model[22] the strain rate of the composite is given by

$$\dot{\varepsilon} = \dot{\varepsilon}_2(1 - V_1)^{2+n_2/2} \tag{7}$$

where $\dot{\varepsilon}_2$ is the strain rate of the deformable matrix, V_1 is the volume fraction of the rigid inclusions, n_2 is the stress exponent of the matrix.

3. Experimental procedure

The starting materials were powders of Al_2O_3 (AKP-53, 99.99% purity, Sumitomo Chemicals Co. Ltd., Japan), $MgAl_2O_4$ (S30CR, 99% purity, Bajkalox, France) and 2 and 3 mol% yttria stabilized teragonal ZrO_2 (2Y and 3Y-TZP, 99.9% purity, Tosoh, Japan). The following types of composites were made: A – Al_2O_3/3Y-TZP, B – Al_2O_3/2Y-TZP and S – $MgAl_2O_4$/3Y-TZP. The basic constituents and several mixtures of these for the composites were ball milled in water. After drying and granulation the plates were obtained by uniaxial pressing at 20 MPa, isostatical pressing at 120 MPa and then sintering for 2 h in air accordingly at 1500, 1600 and 1630 °C for A, B and S composites. From the sintered plates the bars of 1 mm height, 4 mm width and 30 mm length were machined. Some samples were polished and thermally etched at temperatures 50 °C less than the sintering temperature for 1 h in vacuum. The electron scanning microscope micrographs of the etched samples were used for measurements of average grain size by Feret's diameter method.

The creep tests were performed in four-point bending geometry (upper and support span were accordingly 10 and 20 mm) under constant load at 1280 °C using Zwick 1446 universal

Table 1
Grain sizes for composites A (Al_2O_3/3Y-TZP).

Designation	$d_{Al_2O_3}$ (μm)	d_{ZrO_2} (μm)
3Y-TZP		0.47 ± 0.13
28A	0.31 ± 0.06	0.18 ± 0.04
50A	0.30 ± 0.08	0.22 ± 0.19
70A	0.35 ± 0.09	0.27 ± 0.17
86A	0.37 ± 0.19	0.33 ± 0.19
Al_2O_3	0.87 ± 0.49	

All of the composites exhibit densities ≥97% of theoretical density.

Table 2
Grain sizes for composites B (Al_2O_3/2Y-TZP).

Designation	$d_{Al_2O_3}$ (μm)	d_{ZrO_2} (μm)
2Y-TZP		0.48 ± 0.23
10B	0.39 ± 0.12	0.51 ± 0.33
20B	0.46 ± 0.19	0.57 ± 0.36
40B	0.55 ± 0.22	0.42 ± 0.19
60B	0.83 ± 0.19	0.40 ± 0.16
80B	1.14 ± 0.41	0.36 ± 0.12
Al_2O_3	0.87 ± 0.49	

All of the composites exhibit densities ≥99% of theoretical density.

machine. The maximum strain of samples was not more than 2%, but maximum test time was not more than 4 h. Strain rate $\dot{\varepsilon}$ vs. stress σ was calculated from experimental data accordingly to.[23]

4. Results

Scanning electron micrographs of the selected basic components and composites are shown in Fig. 2. Compositions are designated by the volume fraction of Al_2O_3 or $MgAl_2O_4$; for example, 86A contains 86 vol% Al_2O_3 and 14 vol% 3Y-TZP. Average grain sizes with standard deviations are given in Tables 1–3. Microstructure analysis of the composites after testing was not made, but relatively low temperature and small deformation allow us assume that the increase in grain size is negligible. This assumption is supported by the results of[18] where the grain size increase in compression tested Al_2O_3/3Y-TZP composites at temperature 1350 °C (higher than in our case) was insignificant.

Table 3
Grain sizes for composites S ($MgAl_2O_4$/3Y-TZP).

Designation	$d_{MgAl_2O_3}$ (μm)	d_{ZrO_2} (μm)
3Y-TZP		0.47 ± 0.13
10S	0.92 ± 0.40	1.21 ± 0.66
20S	1.03 ± 0.56	1.35 ± 0.57
30S	1.19 ± 0.28	1.10 ± 0.49
40S	1.23 ± 0.34	1.20 ± 0.31
50S	1.05 ± 0.28	0.98 ± 0.19
60S	1.13 ± 0.35	0.97 ± 0.25
70S	1.21 ± 0.74	0.77 ± 0.21
80S	1.81 ± 0.72	0.53 ± 0.18
85S	2.18 ± 088	0.74 ± 0.26
90S	1.97 ± 0.59	0.53 ± 0.14
95S	1.03 ± 0.34	0.56 ± 0.14
$MgAl_2O_4$	1.91 ± 1.71	

All of the composites exhibit densities ≥96% of theoretical density.

The relationships between stress and strain rate were analyzed in log–log scales from which stress exponent n was derived (see Eq. (1)). Values of n as a function of volume fraction of Al_2O_3 or $MgAl_2O_4$ are shown in Fig. 3.

As it is seen that for n varies from 1.4 to 3.0, 1.7 to 2.9 and 1.8 to 3.1 for A, B and S composites, respectively. They are scattered around the value $n=2$ (especially for A and B composites). Hence the results of strain rate measurements for the studied composites are plotted on $(d\varepsilon/dt)^{1/2} - \sigma$ scales (Fig. 4). It is shown in Fig. 4 that the experimental data could be fit by a linear function $(d\varepsilon/dt)^{1/2}$ of σ and that Al_2O_3 and $MgAl_2O_4$ can be treated as a rigid phase (strain rate of the composites decreases as volume fraction of Al_2O_3 or $MgAl_2O_4$ increases).

5. Discussion

The obtained data of superplastic flow measurements of the composites were next analyzed using models presented in Section 2. Fig. 5 presents the plots of the logarithm of strain rate against volume fraction of Al_2O_3 or $MgAl_2O_4$ for A, B and S composites at flow stress of 50 MPa. The curves for isostress, isostrain and rheological model were obtained using end-constituents data (i.e. n_i, $\dot{\varepsilon}_i$, K_i) for Al_2O_3 or $MgAl_2O_4$ ($i=1$) and 2Y-TZP or 3Y-TZP ($i=2$), but for constrained isostrain model experimental data were fit using least-squares method to Eq. (6) with $n=2$ rewritten as:

$$y = V_1(K_1 - K_2) + K_2 \tag{8}$$

where $y = \sigma/\sqrt{\dot{\varepsilon}}$ and $\sigma = 50$ MPa

Values of parameters, including fitting parameters K_1 and K_2 for constrained isostrain model, used for calculating of model curves are placed in Table 4.

Observations of Fig. 5 lead to the following conclusions:

- For composites A for volume fraction of Al_2O_3 $V_1 \leq 0.5$ the experimental points are arranged around the isostress model curve, but for $V_1 > 0.5$ they are arranged around the isostrain and constrained isostrain model curve.
- For the composite B the constrained isostrain model provides the best fit to the experimental data.
- In the case of the composite S proposed models do not practically fit the experimental data.
- The rheological model seems to be useless for the data interpretations.

In order to extend a discussion of the results the comparison of the studied composites was conducted in Fig. 6. It can be seen that strain rates for composites A and S are similar but for B are lower than for A and S. Reason why the strain rate for the composite A is higher than for B is obvious; since composite A grain sizes are smaller than for B. This is why the composites A and S have similar rates of strain will be discussed below.

In order to interpret the results of superplastic deformation measurements of the composites one can hypothesize that the

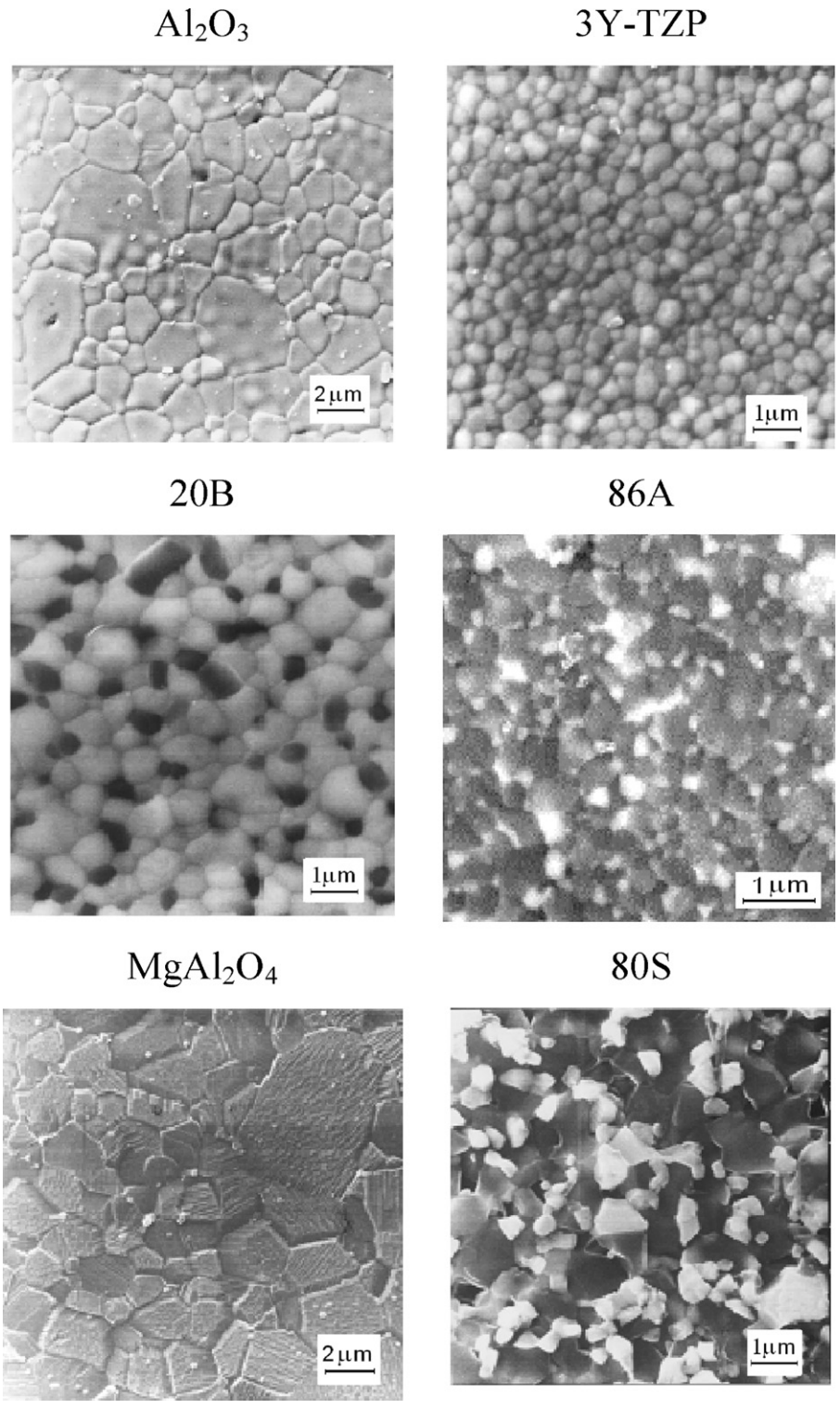

Fig. 2. Scanning electron micrographs of polished and etched surfaces of the selected studied materials. The grains (in composites) with the light shading are 3Y-TZP or 2Y-TZP and the grains with the dark shading are Al_2O_3 or $MgAl_2O_4$.

interaction of the components of both phases, i.e. the diffusion of ions Zr^{4+} and Y^{3+} into Al_2O_3 and $MgAl_2O_4$ grains and Al^{3+} and Mg^{2+} ions into ZrO_2 grains during the sintering process could significantly affect superplastic flow.[17,19] I was shown in[24,25] that the presence of ions Zr^{4+} and Y^{3+} on the grain boundaries of alumina decreases the rate of diffusion of the matrix ions, thus reducing the strain rate of this phase. In turn, in the case of ZrO_2 Al^{3+} and Mg^{2+} ions strengthens the ability of the matrix superplastic deformation,[26–28] but literature data on the diffusion of ions such as zirconium and yttrium into spinel grains and its effects on the superplastic behaviour of this material were not found. Thus strain rate

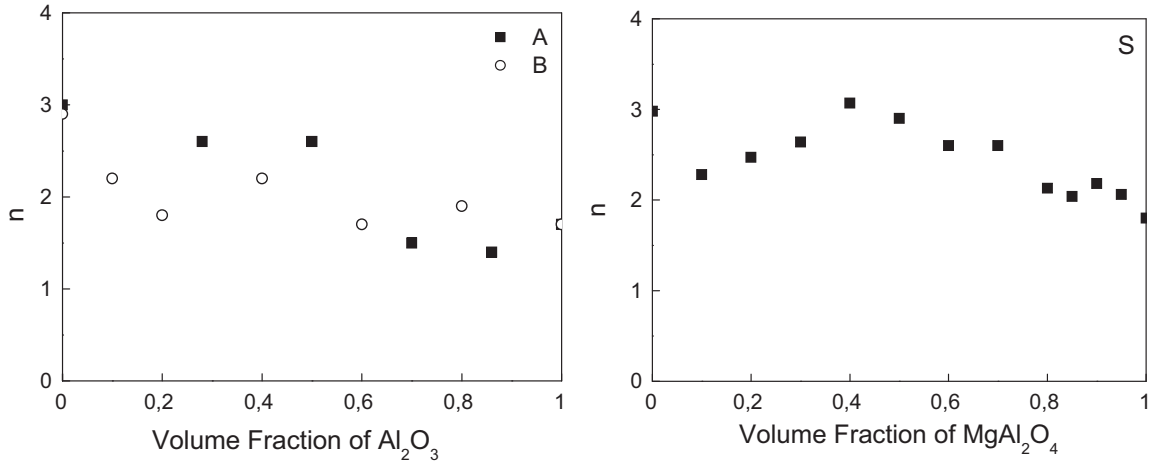

Fig. 3. Stress exponent n as a function of volume fraction of Al_2O_3 or $MgAl_2O_4$ for A, B and S composites at temperature 1280 °C.

cannot be interpreted here simply with the classical rule of mixtures. This is particularly evident in Fig. 5 in the case of composite B, where the average grain size of the composite are comparable with those for the starting materials (see Table 2). The experimental points corresponding to the $V_1 > 0.5$ lie below the isostrain curve. This is probably due to a significant reduction in the superplastic deformation of Al_2O_3 phase caused by diffusion of ions Zr^{4+} and Y^{3+} into alumina grains; for constrained isostrain model strain rate derived for volume fraction of Al_2O_3 equaled 1 is lower than experimentally obtained one for pure Al_2O_3. In the case of composites A smaller grains of the composite in comparison with end-constituents (see Table 1) resulted in the reduction of the effect of strain rate change due to zirconium and yttrium ion diffusion into Al_2O_3 and aluminum ion diffusion into ZrO_2 grains. As it can be seen from Fig. 6, despite the considerable difference of the grain size of composites A and S (see Tables 1 and 3), strain rate of both composites are similar. It means that the spinel/zirconia composite under comparable conditions (like grain size, stress and temperature) is deformed much faster than the corresponding alumina/zirconia compos-

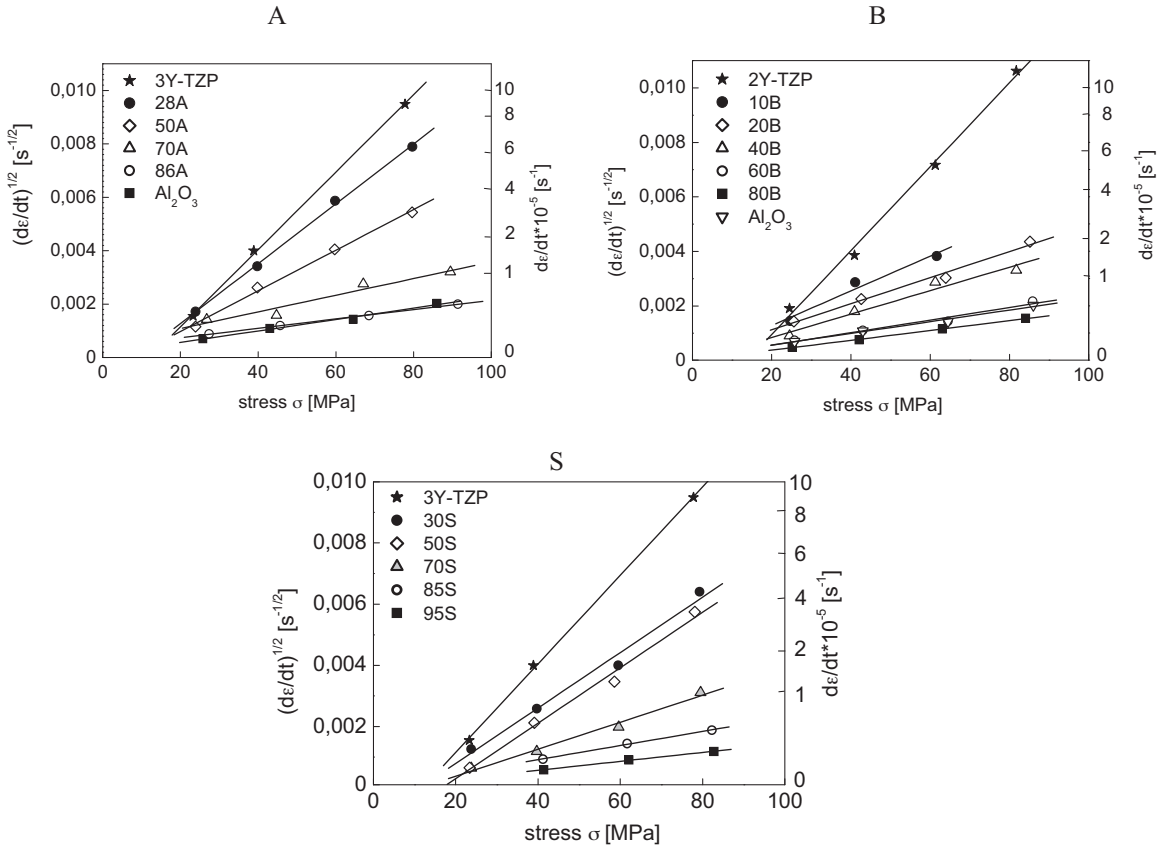

Fig. 4. Square root of strain rate $(d\varepsilon/dt)^{1/2}$ vs. applied stress σ for A, B and S composites at 1280 °C. For sake of clarity the plots for chosen S composites are shown.

Table 4
Parameters for model curves calculations at $\sigma = 50$ MPa and $T = 1280\,^{\circ}C$.

Model	Composite	Parameters					
		n_1	n_2	$\dot{\varepsilon}_1$	$\dot{\varepsilon}_2$	K_1	K_2
Isostress Eq. (2)	A			1.5×10^{-6}	2.7×10^{-5}		
	B			1.5×10^{-6}	3.5×10^{-5}		
	S			1.1×10^{-7}	2.7×10^{-5}		
Isostrain Eq. (4)	A	1.7	3.0			1.28×10^{5}	1.71×10^{3}
	B	1.7	2.9			1.28×10^{5}	1.72×10^{3}
	S	1.8	3.0			3.68×10^{5}	1.71×10^{3}
Constrained isostrain Eq. (6)	A					3.74×10^{4}	4.90×10^{3}
	B					6.50×10^{4}	6.99×10^{3}
	S					5.37×10^{4}	1.12×10^{3}
Rheological Eq. (7)	A		3.0		2.7×10^{-5}		
	B		2.9		3.5×10^{-5}		
	S		3.0		2.7×10^{-5}		

In determining the parameters K_1 and K_2 for the constrained isostrain model all the experimental points with the exception of volume fraction of Al_2O_3 or $MgAl_2O_4$ $V_1 = 1$ are taken into account due to the fact that for all the experimental points and without $V_1 = 0$ and 1 negative (not physical) values of K_2 for the composite S were obtained.

ite. In this situation, it seems that none of the proposed models can explain the behaviour of the composite S because they do not provide the interaction between phases. Increased strain rate of the composite S compared with A and B is caused probably by a significant increase in diffusion coefficient of Zr^{4+} ions in the ZrO_2 grains due to the simultaneous doping with Al^{3+} and Mg^{2+} ions.[28]

Our results are not directly comparable with data from the literature since the latter have been obtained in tensile and compressive tests and at higher temperatures[17,18,20] however, for instance, the conclusions concerning an application of the constrained isostrain model to interpret the results for composite B are the same as in.[18]

Relationships between strain rate and applied stress are presented in Fig. 4 as linear plots of $(d\varepsilon/dt)^{1/2}$ vs. σ. An extrapolation of a straight line to zero strain rate yields the value of σ_0 which could be treated as threshold stress in superplasticity[11,20]; the deformation mechanisms do not work at stresses $<\sigma_0$. The values of σ_0 are shown in Fig. 7 as a function of volume fraction of Al_2O_3 and $MgAl_2O_4$.

The concept of threshold stress has been known for superplastic metallic alloys.[29] A characteristic of the creep behaviour of superplastic metallic alloys is the experimental observation that the relationship between the strain rate and the applied stress at constant temperature is often sigmoidal. This sigmoidal relationship is manifested by the presence of three distinct deformation regions[29]: region I – the low-stress region (the stress exponent, $n > 2$); region II – intermediate-stress region (n is close to 2); region III – the high-stress region ($n > 2$). It was suggested[29] that the transition in behaviour between region I and II may not necessarily reflected a change in deformation mechanism but can arise from the presence of a threshold stress σ_0 which decrease strongly with increasing temperature. Physical meaning of this concept: it is the minimal force per unit area required for grains to displace with respect to each other. If σ_0 exists then $d\varepsilon/dt \sim (\sigma - \sigma_0)^n$. The possible origin of σ_0 for superplasticity in metallic alloys is impurity segregation at grain boundary and their interaction with grain boundary dislocation.[29] For yttria-stabilized tetragonal zirconia polycrystals two different explanations of the origin of the threshold exist:

1. It was established in[30,31] that grain-boundary segregation of yttrium caused an appearance of the threshold stress in this ceramics. This segregation changes the chemical composition as well as space charge at the boundaries, creating a local electric field, consequently affecting grain boundary sliding (GBS) which is responsible for the superplastic flow. GBS is accommodated by lattice diffusion of cations.
2. In turn in[20] it was claimed that the threshold stress could be ascribed to the nucleation of intragranular dislocations, which contributed to the relaxation of stress concentrations exerted around the grain junctions and boundary ledges by GBS. The strain rate is controlled by the rate of the dislocation recovery process limited by the lattice diffusion of cations.

Analyses of presented in this paper results do not allow to assess which of the models of σ_0 origin is correct. It is seen in Fig. 7 that σ_0 decreases as a function of Al_2O_3 content to zero for composite A for alumina content above 0.5. However for composite B all σ_0 values (with an exception of 2Y-TZP) are close zero. For composite S, up to content of $MgAl_2O_4$ of 0.7, σ_0 is almost constant and next decreases to zero up to 0.85. Papers [20,32] point out that the threshold stress effect is measured not only for zirconia ceramics but also for spinel–zirconia composites (even with large content of spinel phase). In turn in[30] it was claimed that no threshold stress should be measured if there was no segregation or charge effect. As an example alumina ceramics was given there. In alumina ceramics in which no segregation at the grain boundaries was described no threshold stress existed. The same situation was in yttria doped alumina in which yttrium segregation took place at the boundaries the effective electric charge of the dopants (compared with the par-

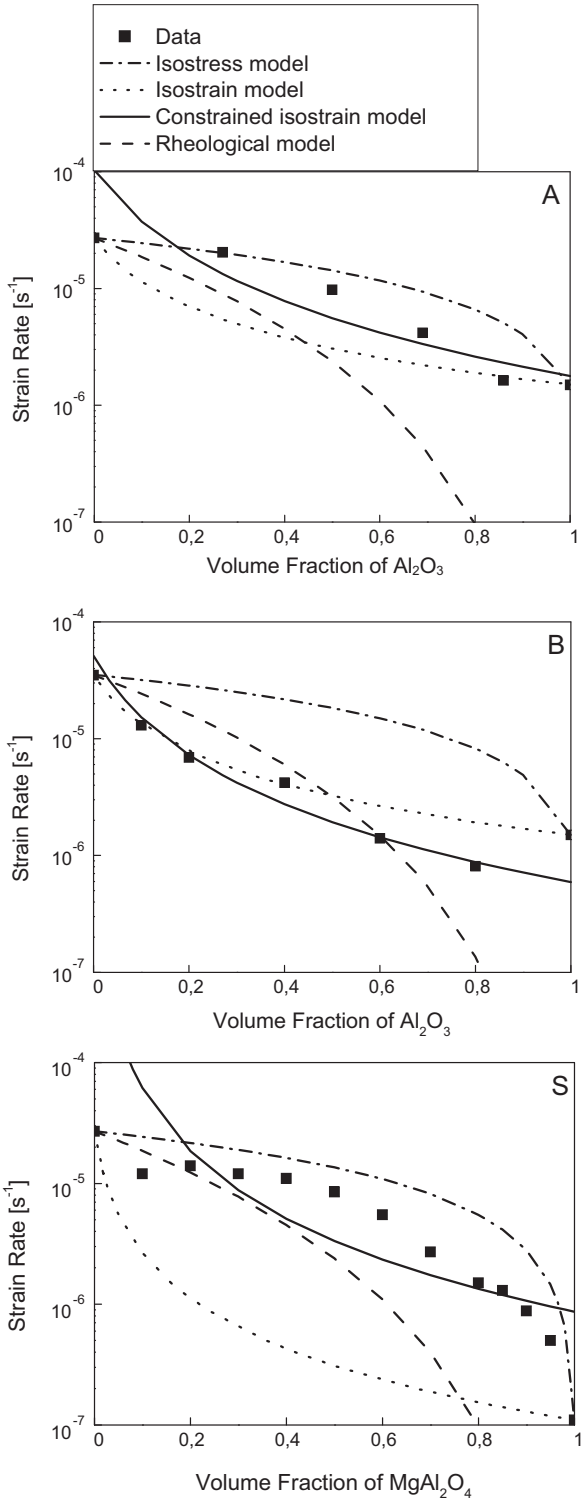

Fig. 5. Strain rate plotted as a function of volume fraction of Al_2O_3 and $MgAl_2O_4$ for studied composites A, B and S at stress 50 MPa and temperature 1280 °C.

ent ion) was zero, no charge effect was expected. In consequence no threshold stress should be measured. The cited reports support the thesis that threshold stress phenomenon is significant for spinel–zirconia composites but disappears in alumina–zirconia composites as it is observed in the case of A and B composites (Fig. 7).

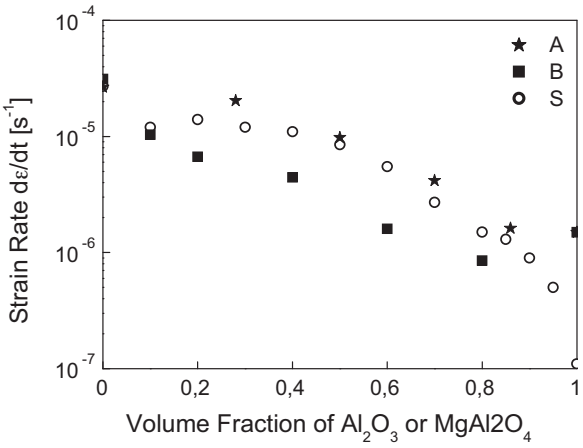

Fig. 6. The comparison of strain rates plotted as a function of volume fraction of Al_2O_3 or $MgAl_2O_4$ for studied composites A, B and S at stress 50 MPa and temperature 1280 °C.

Value of σ_0 obtained here for 3Y-TZP and for 2Y-TZP 12.0 and 13.8 MPa respectively are consistent with σ_0-value predicted using $\sigma_0 = (5 \times 10^{-4}/d)\exp(120{,}000/RT)$.[11] The calculated hence values are 11.6 and 11.4 MPa respectively for 3Y-TZP and 2Y-TZP. In turn, σ_0-value obtained by extrapolation to temperature 1280 °C of the relationship for 30 vol% $MgAl_2O_4$/3Y-TZP in[20] is about 30 MPa. It is higher than obtained here for the same composites (11.3 MPa). It probably stems from the fact that the grain sizes in[20] are much smaller than in our case (they are 0.3 and 0.35 μm for 3Y-TZP and $MgAl_2O_4$, respectively, but in our case they are 1.1 and 1.2 μm). This relatively high level of σ_0 for significant content of spinel in spinel/zirconia composites is interpreted in[20] as caused by enhanced diffusivity in zirconia which can more effectively relax the stress concentration around grain junctions, so that higher stresses are necessary to exert stress concentrations sufficient to nucleate dislocations in the spinel/zirconia composites.

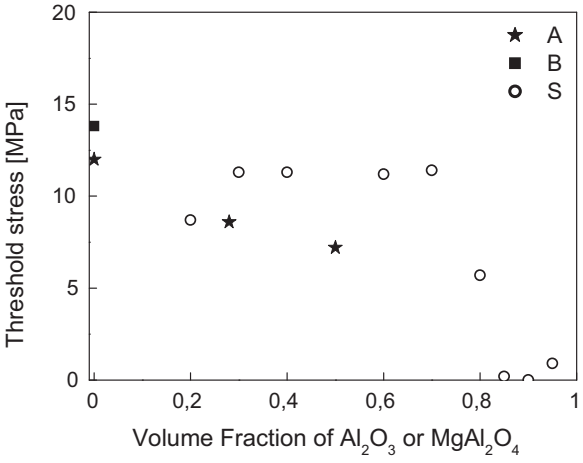

Fig. 7. The threshold stress for studied composites A, B and S at temperature 1280 °C plotted as a function of volume fraction of Al_2O_3 or $MgAl_2O_4$.

6. Conclusions

In the present paper the results of superplastic flow measurements of Al_2O_3/3Y-TZP (A), Al_2O_3/2Y-TZP (B) and $MgAl_2O_4$/3Y-TZP (S) particle composites at temperature 1280 °C have been reported. The results can be summarized as follows:

- Values of stress exponent n are scattered around $n = 2$ for A and B composites and they are in the range of 1.8–3.1 for S composites.
- The strain rate of the composites decreases as a function of Al_2O_3 or $MgAl_2O_4$ content.
- Composites S show greater susceptibility to superplastic deformation than A and B.
- Isostress, isostrain and constrained isostrain model can predict successfully the superplastic behaviour of A and B composites but not of S. In turn, the rheological model seems to be useless for the data interpretations.
- The threshold stress approach can be applied for describing superplastic flow of S composites but it seems to be rather unsuitable for A and B composites.

References

1. Munro RG. Evaluated material properties for sintered α-alumina. *J Am Ceram Soc* 1997;**80**(8):1919–28.
2. Yano T. Effects of neutron irradiation on the mechanical properties of magnesium aluminate spinel single crystals and polycrystals. *J Am Ceram Soc* 1999;**82**(12):3355–64.
3. Ge QL, Lei TC, Zhou Y. Microstructure and mechanical properties of hot pressed Al_2O_3–ZrO_2 ceramics prepared from ultrafine powders. *Mater Sci Technol* 1991;**7**:490–4.
4. Tuan WH, Chen RZ, Wang TC, Cheng CH, Kuo PS. Mechanical properties of Al_2O_3/ZrO_2 composites. *J Eur Ceram Soc* 2002;**22**:2827–33.
5. Fujita M, Yoshimatsu H, Osaka A, Miura Y. Preparation and properties of ZrO_2 dispersed MgO–Al_2O_3 ceramics (Part 2) – effects of ZrO_2 content. *J Ceram Soc Jap Int Ed* 1995;**103**:825–30.
6. Ganesh I, Ferrita JMF. Synthesis and characterization of $MgAl_2O_4$–ZrO_2 composites. *Ceram Int* 2009;**35**:259–64.
7. Cutler RA, Reynolds JR, Jones A. Sintering and characterization of polycrystalline monoclinic, tetragonal, and cubic zirconia. *J Am Ceram Soc* 1992;**75**(8):2173–83.
8. Stevens R. Introduction to zirconia. Zirconia and zircinia ceramics. Magnesium Electron Ltd.; 1986.
9. Choksi AH, Mukherjee AK, Langdon TG. Superplasticity in advanced materials. *Mater Sci Eng* 1993;**R10**:237–74.
10. Wakai F, Sakaguchi S, Matsuno Y. Superplasticity of yttria-stabilized tetragonal ZrO_2 polycrystals. *Adv Ceram Mater* 1986;**1**(3):259–63.
11. Jiménez-Melendo M, Dominguez-Rodriguez A, Bravo-Leon A. Superplastic flow of fine-grained yttria stabilized zirconia polycrystals: constitutive equation and deformation mechanisms. *J Am Ceram Soc* 1998;**81**(11):2761–76.
12. Owen DM, Chokshi AH. The high temperature mechanical characteristics of superplastic 3 mol% ytttria stabilized zirconia. *Acta Mater* 1998;**46**(2):667–79.
13. Charit I, Chokshi AH. Experimental evidence for diffusion creep in the superplastic 3 mol% yttria-stabilized tetragonal zirconia. *Acta Mater* 2001;**49**:2239–49.
14. Kottada RS, Chokshi AH. The high temperature tensile and compressive deformation characteristics of magnesia doped alumina. *Acta Mater* 2000;**48**:3905–15.
15. Morita K, Hiraga K, Kim B-N, Suzuki TS, Sakka Y. Strain softening and hardening during superplastic-like flow in a fine-grained $MgAl_2O_4$ spinel polycrystals. *J Am Ceram Soc* 2004;**87**(6):1102–9.
16. Wakai F, Kato H. Superplasticity of TZP/Al_2O_3 composite. *Adv Ceram Mater* 1988;**3**(1):71–6.
17. Clarisse L, Baddi R, Bataille A, Crampon J, Duclos R, Vicens J. Superplastic deformation mechanisms during creep of alumina–zirconia composites. *Acta Mater* 1997;**45**(9):3843–53.
18. Wang J, Taleff EM, Kovar D. High-temperature deformation of Al_2O_3/Y-TZP particulate composites. *Acta Mater* 2003;**51**:3571–83.
19. Morita K, Hiraga K, Sakka Y. High-strain-rate superplasticity in Y_2O_3-stabilized tetragonal ZrO_2 dipersed with 30 vol% $MgAl_2O_4$ spinel. *J Am Ceram Soc* 2002;**85**(7):1900–2.
20. Morita K, Hiraga K, Kim BN. High-strain rate superplastic flow in tetragonal ZrO_2 polycrystal enhanced by the dispersion of 30 vol.% $MgAl_2O_4$ spinel particles. *Acta Mater* 2007;**55**:4517–26.
21. French JD, Zhao J, Harmer MP, Chan HM, Miller GA. Creep of duplex microstructures. *J Am Ceram Soc* 1994;**77**(11):2875–965.
22. Yoon CK, Chen I-W. Superplastic flow of two-phase ceramics containing rigid inclusions-zirconia/mullite composites. *J Am Ceram Soc* 1990;**73**(6):1555–65.
23. Hollenberg GW, Terwillinger GR, Gordon RS. Calculation of stresses and strains in four-point bending creep tests. *J Am Ceram Soc* 1971;**54**(4):196–9.
24. Wakai F, Nagano T, Iga T. Hardening in creep of alumina by zirconium segregation at the grain boundary. *J Am Ceram Soc* 1997;**80**(9):2361–6.
25. Yoshida H, Ikuhara Y, Sakuma T. High-temperature creep resistance in rare-earth-doped, fine-grained Al_2O_3. *J Mater Res* 1998;**13**(9):2597–601.
26. Nakatani K, Nagayama H, Yoshida H, Yamamoto T, Sakuma T. The effect of grain boundary segregation on superplastic behavior in cation-doped 3Y-TZP. *Scr Mater* 2003;**49**:791–5.
27. Miramuda J, Nakano M, Sasaki K, Ikuhara Y, Sakuma T. Effect of cation doping on the superplastic flow in yttria-stabilized tetragonal zirconia polycrystals. *J Am Ceram Soc* 2001;**84**(8):1817–21.
28. Boniecki M, Natanzon Y, Łodziana Z. Effect of cation doping on lattice and grain boundary diffusion in superplastic yttria-stabilized tetragonal zirconia. *J Eur Ceram Soc* 2010;**30**:657–68.
29. Mohamed AH. Interpretation of superplastic flow in terms of a threshold stress. *J Mater Sci* 1983;**18**:582–92.
30. Gómez-Garcia D, Lorenzo-Martin C, Muñoz-Bernabé A, Dominguez-Rodriguez A. Correlation between yttrium segregation at the grain boundaries and the threshold stress for plasticity in yttria-stabilized tetragonal zirconia polycrystals. *Philos Mag* 2003;**83**(1):93–108.
31. Dominguez-Rodriguez A, Gómez-Garcia D, Lorentzo-Martin C, Muñoz-Bernabé A. Influence of the yttrium segregation at grain boundaries in the superplasticity of yttria tetragonal zirconia polycrystals. *J Eur Ceram Soc* 2003;**23**:2969–73.
32. Addad A, Crampon J, Duclos R. High temperature deformation of a 5 wt.% zirconia–spinel composite: influence of a threshold stress. *J Eur Ceram Soc* 2002;**22**:329–35.

Glossary

A_0: dimensionless constant in the creep equation
b: Burgers vector
d: grain size
D: diffusion coefficient
G: shear modulus
k: Boltzmann's constant
$K_i = G(kT/A_0DGb)^{1/n_i}(d/b)^{p/n_i}$
n: stress exponent
p: inverse grain size exponent
T: temperature
V_I: volume fraction of rigid phase (Al_2O_3 or $MgAl_2O_4$)
y: $\sigma/\sqrt{\dot{\varepsilon}}$
$\dot{\varepsilon}$: $d\varepsilon/dt$ – strain rate
σ: applied stress